

Article

Effect of Artificial Aging Treatment and Lubrication Modes on the Machinability of A356 Cast Alloys

M.A. Alliche¹, A. Djebara^{1*}, Y. Zedan² and V. Songmene²

¹ Department of Mechanical Engineering, ENPC, Constantine, Algeria

² Departments of Mechanical Engineering, ÉTS, Montreal, Canada

* abdelhakim.djebara@enp-constantine.dz

Abstract: This article discusses the effects of heat treatment and lubrication modes on the machinability of Al-Si-Mg alloys (A356) cast alloys for as-received alloy, solution heat-treated alloy (SHT) as well as solution heat treated and then aged alloys at 155°C, 180°C, and 220°C. In the course of machinability evaluation, several criteria including cutting force, surface roughness, tool wears and burr analysis (chip) were studied. The results and analysis in this work indicated that selected machinability criteria are important and necessary to effectively evaluate the machinability of A356 alloys. Machinability of both materials and tool was estimated in terms of chip thickness ratio and burr formation, roughness, cutting force and flank wear. The effects of various lubrication modes such as dry, mist and wet, cutting parameters, including cutting speed and feed rate on the machinability of A356 cast alloys were also examined. Experimental results prove that the heat treatment parameters strongly control the burr formation and surface quality. The results obtained indicate that better drilling performance in terms of surface quality occurs at high feed rate, dry drilling and artificial aging at T6.

Keywords: aluminum alloys; artificial aging; drilling; surface quality; cutting fluid; burr formation

1. Introduction

Using aluminum alloys as replacement of steels is expected to lead to great progress in saving energy, life-cycle cost and recyclability [1]. Advanced aluminum materials have been widely used in the automobile industry for manufacture of several types of car parts, such as wheels, panel and even in the vehicle structure [2]. Aluminum alloys have progressively more attracted the attention of many specialists, designers and engineers as promising structural materials for aerospace applications and automobile industry [3]. However, it is necessary to improve the strength and the formability of aluminum alloys for further industrial applications [4].

The most common metal cutting process used is drilling. The drilling processes of Al-Si-Mg alloys are carried out with some difficulties. These materials tend to form burrs and adhere to the tool surface as result of plastic deformation in machined parts [5]. Burrs are formed on the part edges [6]. Output burrs is important as it is more difficult to remove because of their large sizes, which in fact require higher precision deburring and edge finishing tools. Therefore, more attention has been paid to drilling exit burrs than entrance burrs [7]. Product quality without burrs is an important parameter in drilling that increases reliability and performance. Limit the burr formation at the source is a better solution than deburring them in a subsequent finishing operation [8]. Sofronas summarized several cutting factors that contribute to drilling burr formation [9]. According to his survey, the most effective factors are drilling geometry, material of workpiece, machining rigidity, drilling condition and cutting fluids. Hasegawa et al examined burr formation based on cutting speed, feed rate, and drill geometry [10]. According to Hasegawa et al, there is a formation of small burrs for high speed. Furthermore, it was exhibited that lower feed rate lead to decreased burr size. Pande and Relekar determined that a smaller burr height results from the use of a drill tool diameter

in range of 8-10 mm [11]. This study was based on the influence of drill diameter, feed rate, length to diameter ratio, and material hardness on burr height and thickness. The study of the drilling burr formation morphology by Ko and Lee showed that the burr thickness is independent of the feed rate. On the other hand, the material properties have significant effects on the burr thickness than feed rate [12].

In the literature, the role of artificial aging has extensively reported in relation to the alloys machinability [13, 14]. It was also found that minimum values of exit burrs are due to the material hardness in range of 130-140 BHN. According to Gillespie, hard materials tend to reduce the size of burrs because the material is more likely to crack close to the cutting edge [15]. Similar findings as Gillespie were found by Ko [16]. The A356 aluminum alloy belongs to the Al-Si-Mg series which can be heat treated. Owing to the presence of magnesium content in these alloys, magnesium combines with Si to form a hard phase by Mg₂Si precipitation [17]. Heat treatment increases the hardness, improves the surface finish of the workpiece by reducing the built-up-edge (BUE) formation on the tool. In drilling and turning operations, any increase in the cutting temperature is critical to tool life since it produces excessive accelerated heat-causing wear-out of the edge [18]. Typical automotive machining techniques, however, usually require a minimum of workpiece hardness in order to avoid potential complications associated with built-up edge (BUE) on the tool. A minimum hardness of 80 BHN is desirable for most automotive machine shops [19, 20]. As a courtesy to this observation, the 319 aluminum alloy intake manifolds are often aged to the T5 temper, and the 356 aluminum alloy manifolds usually require full artificial aging treatment to the T6 temper [13, 21].

To overcome the restrictions imposed against wet machining, special attentions have been paid to use of dry machining over the past few years. In addition, the use of cutting fluids increases the machining cost approximately 16% of production costs and degrades the environment. However, sometimes it is still requested to use the wet machining, especially under extreme cutting conditions when better surface finish quality and higher machining efficiency are required. Since few years ago, a new technique known as minimum quantity of lubricant (MQL) has been proposed to insert the fluid/lubricant in the form of an aerosol spray at a rate not exceeding 100 ml/h (atomized format to form fine droplets) [22, 23]. The successful applications of MQL in drilling operations are reported in literature [24-26]. Distinctly from the effectiveness of the MQL on machining imperfections reduction, additional studies are still required to select appropriate cutting conditions to reduce machining imperfections over a limited range of process parameters [27]. Sreejith and Ngoi statement the effects of flooded coolant, MQL and dry conditions on surface roughness, tool wear and cutting forces in turning aluminum alloy [28]. It was established that MQL can replace the flooded coolant condition when properly employed.

Machining parameters such as tool type, depth of cut, cutting speed, feed rate, ductility, hardness and strength are the most important elements to control the machinability of aluminum alloys (fundamental and extrinsic) [29]. To better analyze the effects of heat treatment methods on machinability attributes, the parts were machined under controlled cutting conditions after heat-treated to produce different precipitation states. The main objectives of this study were focused on evaluating the influence of machining conditions and cutting fluid on the surface roughness, cutting force and burr formation when drilling A356 under several heat treatment conditions. This would enable us to define better the machinability of A356.

2. Materials and Methods

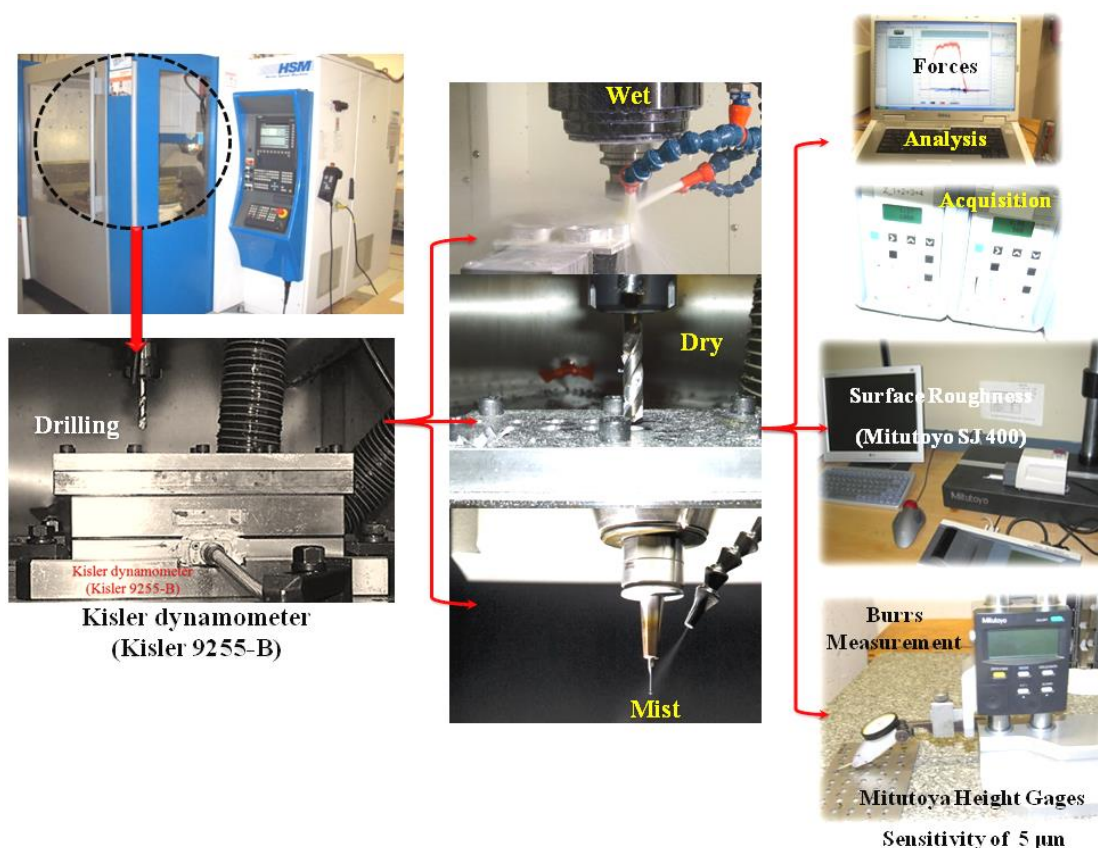
Machining tests were conducted on a 3-axis CNC milling machine (50 kW, 28000 rpm, 50 Nm) using uncoated HSS twist drills (10 mm stub drill bright finish with 118° degree conventional point). It is to underline that similar drilling tools were used during the tests in order to ensure the reliability of geometry, microstructure and properties of the tools used. The work materials were A356 cast alloy blocks (300 × 100 × 20 mm), mounted on a special machining fixture (Figure 1). All samples (work materials) were solution heat-treated at 540°C, for solution period of 8 hours. The solution-heat treated samples were then quenched in warm water (60°C). The chemical composition of the work part used (A356) is presented in Table 1.

Table 1. Chemical composition of A356 alloy

	Silicon	Copper	Magnesium	Fe	Manganese	Zinc	Ti	Al
	Min-Max	Max %	Min-Max %	Max %	Max %	Max	Max	
A356	6.5-7.5	0.2	0.245-0.25	0.2	0.1	0.1	0.2	Balance

The work parts were received in as-cast state (T0), and the work parts were divided into five groups as following:

- 2 blocks in as-cast state (T0);
- 2 blocks in T4 condition (Solution Heat-Treated "SHT"+ Quenching);
- 2 blocks in T61 condition (SHT → quenching → artificial aging at 155°C for 5 hours);
- 2 block in T62 condition (SHT → quenching → artificial aging at 180°C for 5 hours);
- 2 blocks in T7 condition (SHT → quenching → artificial aging at 220°C for 5 hours).

**Figure 1.** Experimental setup used

Cutting forces were measured using a Kistler 9255B table dynamometer. The cutting forces were then amplified and analyzed using the sampling frequency of 48 KHz. The drilling performance was estimated based on the total drilling force (F_t). The average thrust force generated during the drilling of each hole was calculated within the time period corresponding to the drilling cycle. The surface roughness of each hole was estimated according to the R_a parameter using the Mitutoyo SJ 400 profilometer. In order to examine the surface texture of drilled holes, the samples were ultrasonically cleaned with ethanol. The surface roughness was recorded at four dissimilar positions (90° apart) and the measurements were repeated twice at each point. The average value was used for analysis purposes in this study.

Chips were studied for each experiment, after preparation for further metallographic examinations. The Hitachi scanning electron microscope (SEM) S-3600N was used to capture the

high resolution images of the chip morphology were collected for each experiment and tool wear. To that end, the samples were ultrasonically cleaned with ethanol bath before being transferred to SEM microscope. The burr height was measured using Mitutoyo height gauges ($\pm 5 \mu\text{m}$). To measure the burr height, the gauge indicator was first placed on the datum surface and then measured to the top end of the burr. The distance between the two measurements was considered as the burr height. The average value of the measurements was obtained with a four-fold repetition, and then it was used as the burr size in experimental analysis. The burr formation morphology was monitored using a high resolution optical microscope.

In the current research, drilling tests were performed for various coolant application modes, at different cutting speeds and feed rates. To formulate relationship between the machining responses and cutting parameters and their interactions effects, a full factorial design of experiment was used to generate the matrix of experiments. To that end, three lubrication modes and five heat treatment methods were used in combination with three levels of cutting speed and feed rate. The factors studied and their levels are summarized in Table 2. The drilling tests were replicated four times for each condition. Totally 135 experiments were conducted to complete the study.

Table 2. Design of experiment factors and their levels

Variable parameter	Min limit		Intermediate limit		Max limit
A: Cutting speed (m/s)	2 000		6 000		10 000
B: Feed rate (mm/rev)	0.015		0.15		0.35
C: Heat treatment	T ₀	T ₄	T ₆₁	T ₆₂	T ₇
D: Lubricant mode	Dry		Mist		Wet

3. Results and Discussion

3.1. Microstructure

Generally, the limited solubility of Si in aluminum structures an Al-Si eutectic system. The main components are the major alpha-Al solid solution phase and the Al-Si eutectic. Figure 2.1 shows the microstructure of the base alloy in the as-cast condition. The types of phases which are present in the microstructure are clearly revealed. The primary Al-matrix, the eutectic silicon particles are seen as wide and irregular structures and few and asymmetrical phases of Mg₂Si. For the most part, the Al-Si casting alloy proprieties were governed by the shape of the silicon particles. After a certain period of heating Al-Si-Mg alloys at elevated temperature (540oC), shape perturbations in the silicon particles begin to appear until, eventually, the particles are broken down into a series of spherical crystals. This stage is called the fragmentation stage. Consequently, the Si particle size begins to increase as a result of particle coarsening if its size is greater than the critical volume. This stage is called the coarsening stage as shown in Figure 2.2. With solution heat treatment, the Mg₂Si can be dissolved into the aluminum matrix, the solubility being dependent on the solution temperature. Considering the different stages of heat treatment, we find that the fragmentation and coarsening stages can also occur simultaneously, in the same microstructure, depending on the variety of Si particle sizes present in the as-cast structure. Accordingly, some longer particles may be fragmented, other smaller Si particles may become spheroidized and those already spheroidized could start coarsening, at any particular time during the solution treatment process.

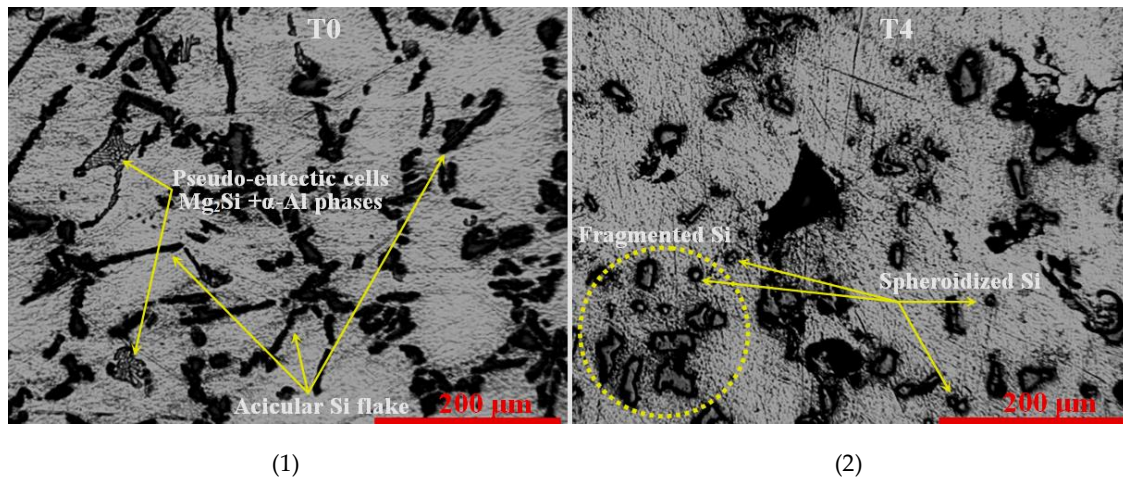


Figure 2. Effect of solution heat treatment on the eutectic Si particle observed in A356 in (1) A356-T0: As-received (2) A356-T4: After SHT at 540°C for 8 h

Cast Al-Si alloys are commonly heat treated to various tempers depending on the application requirements. The most regular heat treatment temper for mechanical parts is the T6 for ambient service temperatures and the T7 temper for higher temperature applications. Heat treatment is expected to impart significant microstructural changes as revealed in Figure 3. Figure 3.1 and 2 shows the morphological characteristics of the Si particle observed in aged-T6 and stabilized/over aged-T7 samples of A356 cast alloys. When the temperature increased to 155 and 220 °C, respectively producing the T6 and T7 aging, the morphology of Si particles marks the beginning of the coarsening process. In the A356-T6 condition, the Si particles were Rod-like formed. Applying the A356-T7 state result in the Rod-like Si particles, which undergo necking; followed by fragmentation, as can be seen in Figure 3.2 for a sample treated at 220°C for 5 hours. Subsequently quenching can lock the Si particles within the aluminum matrix to form a supersaturated solid solution. In this alloy, necking and rod-like eutectic Si particles are observed. However some of the eutectic silicon particles still possess coarse acicular shape. The size of eutectic silicon particles are seen in this microstructure as large eutectic-Si particles when this microstructure is compared to as-cast. The morphological characteristics of the Si particle have an influence on the mechanical properties, where a transform from an acicular to a fibrous morphology improves the mechanical properties and the ductility. The Mg₂Si phase observed in the as-cast condition seem to have disappeared after heat treatment. The solution temperature is the key factor in this regard, and must be high enough so that the Mg₂Si can fully dissolve in solution.

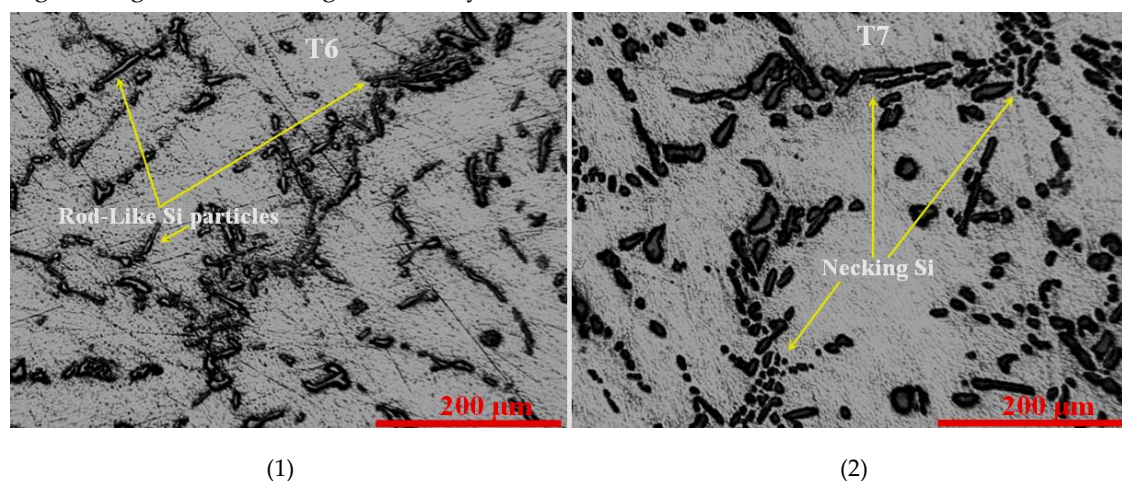


Figure 3. Effect of SHT on the eutectic Si particle observed in A356 in (1) A356-T6: SHT → quenching → artificial aging at 155°C for 5 hours (2) A356-T7: SHT → quenching → artificial aging at 220°C for 5 hours

3.2. Cutting Force

Figure 4 establishes the effect of cutting speed and feed rate conditions on the thrust force during dry, mist and wet drilling applications of A356 heat treated. Thrust force variation was found to be considerably lower relative to cutting speed. The cutting speed impact is more important on increasing of the thrust force value. The results also reveal that as the feed rate increases, the thrust force increases considerably. As expected, the thrust force is smaller with lower feed. For feed rate above 0.015 mm/rev the thrust force increase at a much higher rate. All forces amplified with a high rate when the feed rate is extremely high. It was also found that for all feed rate and heat treatment, dry cutting engendered higher thrust force in opposition to mist and wet modes mostly due to the BUE on the cutting tool. In the T6 case, it was found that for all cutting speeds, wet cutting engendered higher cutting force in opposition to dry and mist modes for the most part due to the cutting tool wears. The wet mode influence is insignificant on the thrust force values similar to all other factors except for the feed rate factor.

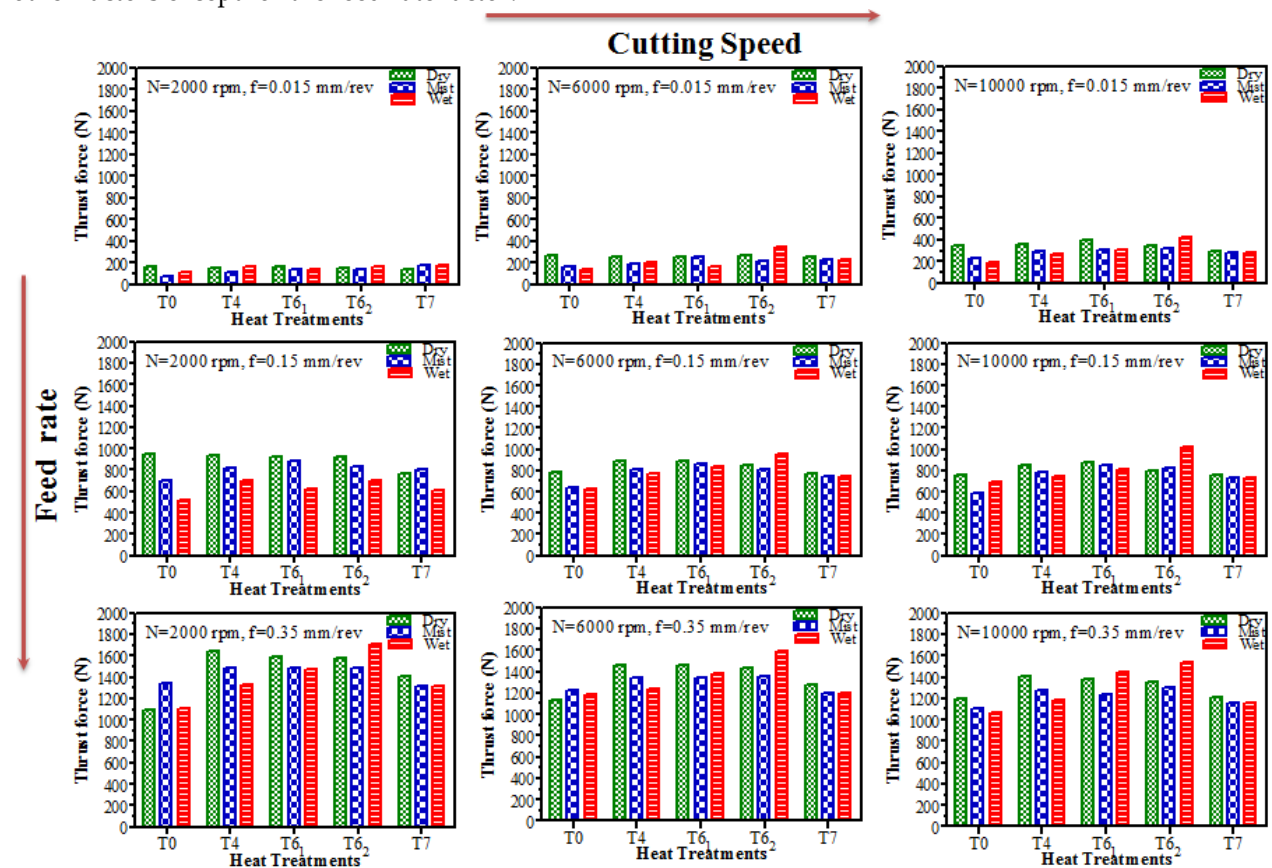


Figure 4. Effect of cutting speed and feed rate conditions on the thrust force during dry, mist and wet drilling of A356 heat treated

3.3. Chip Characterization

After examining the morphology of the chips morphology, we considered that segmented chips are typical for aluminum alloys as shown in Figure 5. The chips produced by drilling of the A356-T0 cast alloys have many small cracks that characterize brittle fracture (Figure 5.1). Unlike for A356-T4 which is more ductile, chip formation does not reveal this type of crack (Figure 5.2). Compared to the case of brittle materials, deformation and friction on the chip surface are more elevated. At the lower feed rate, the chip structure shows a high plastic deformation and it is more deformed and lengthened. Consistently, at low feed rate the plastic strain exists over most of the chip area and the adiabatic shear is less pronounced. The chips produced by drilling of A356-T6 show no systematic segmentation. It was noticed that the fragmentation bands are denser, as shown in Figure 5.3, although the bands are strongly crushed in the heat treatment case of T7 (Figure 5.4). At the higher

feed rate, the shear strain in the primary shear zone is insignificant which results in the smaller chip deformation. This can be explained by the medium thermal conductivity of aluminum, which leads to an increase in shear plane temperature and softening of the material, and this result more strain in the same shear plane. Furthermore, at higher feed, the bulk of the segment seems to be displaced with elevated strain at the adiabatic shear zone, and very small strain in the bulk of the segment area. In this situation, the chip formation is with cyclic segment and adiabatic shear lines delimiting each segment.

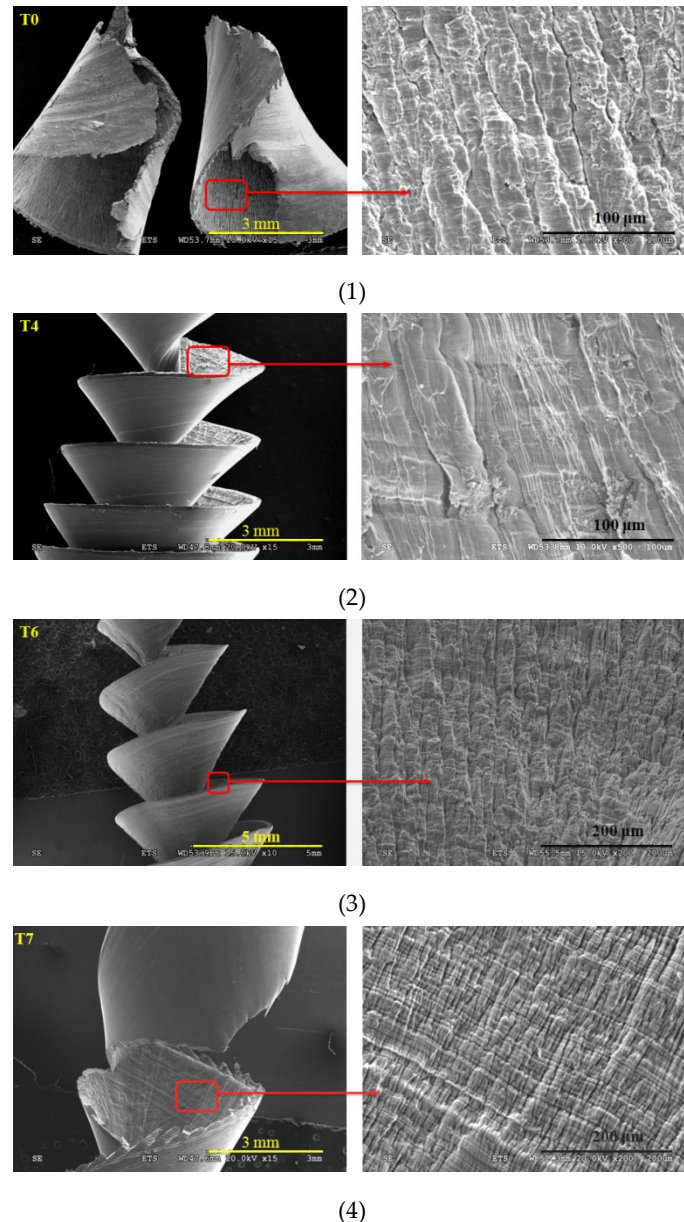


Figure 5. Effect of heat treatment on chips segmentation produced by drilling of the A356 (1) As- received (2) After SHT at 540°C for 8 h (3) at 155°C for 5 hours (4) at 220°C for 5 hours

Drilling is performed with uncoated HSS twist drills. The measurement of the chip-forming effect is specified by the chip compression ratio. The significance of chip compression ratio is to provide information on the rate of plastic deformation and evaluate the temperature distribution in the chip formation zone during drilling process in our case. An elevated shear angle indicates a lower chip compression ratio value, which is reflected by low strain in the chip and reduced energy consumption. The chip compression ratio is the ratio of the chip thickness to the depth of cut (Eq. 1). Tool geometry was designed to remove a cut with the thickness h_1 (uncut chip thickness) and the

produced chip has a thickness of h_2 (actual chip thickness). The chip compression ratio ζ can be defined as:

$$\zeta = h_2/h_1 \quad (1)$$

Figure 6.1 and 2 shows the control of cutting speed and feed rate on the chip compression ratio in dry, mist and wet drilling of heat-treated A356. Commonly, the chip compression ratio drops drastically with increasing artificial aging temperature (T61). Then, it increases according to this artificial aging temperature (T62, T7). The values of the chip compression ratio for the same feed rate are very close for all the cutting speeds studied. The scatter in the chip compression ratio with increasing cutting speed is not high for same feed rate. On the other hand, there is a considerable decreasing in chip compression ratio with increasing feed rate. It is also noted with large values of feed rate results a decrease in the chip compression ratio due to the decrease of the plastic deformation zone. Also, the variation in the chip compression ratio for the identical cutting speed of drilling of the A356 as-received, after heat treatment in solution and T61. In the T62 and T7 conditions, the decrease in chip compression ratio is low and has a tendency to increase. Lubrication modes must be chosen based on the drilling parameters used for a given combination of tools and material. However, for mist lubricant mode, the chip compression ratio shows two different evolutions for the three feed rate used. For low values of feed rates, the chip compression is significant for mist compared to other lubrication modes. On the other hand, for high values of feed rates, the chip compression is significant for dry compared to other lubrication modes. This is attributed to the chip segmentation as discussed earlier (adiabatic shear and plastic strain). Also, the variation in the chip compression ratio is more pronounced for lower feed rates and for various cutting speeds. The contact length between the tool and chip has been greatly increased when the feed rate is increased. In addition, the friction coefficient value decreases as the cutting speed increases, due to the increase in tool-chip contact, which produces a thermal softening and thus decreases the friction coefficient. Then, it is evident that the tool-chip friction contact decreased as the cutting speed and feed rate increased for all cases. However, an elevated ratio of chip compression at a low feed rate increases the normal load, which increases the friction coefficient. Under these conditions, the effect of the feed rate plays a central position in drilling performance.

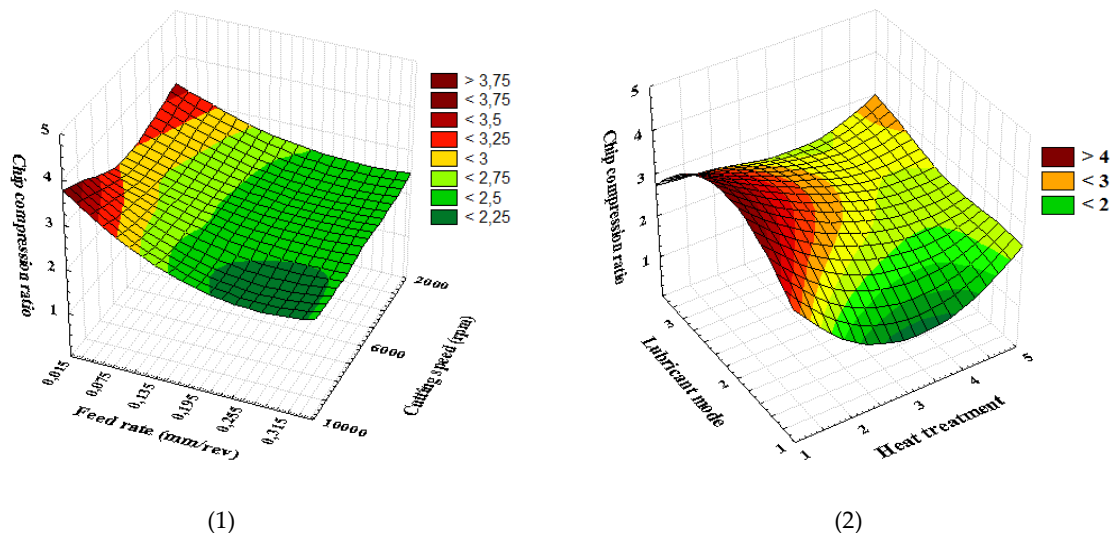


Figure 6. Control of cutting speed and feed rate on chip compression ratio in dry, mist and wet drilling of heat-treated A356

3.4. Surface Quality

Surface finish of the machined parts is a very important result in mechanical manufacturing. This aspect affects the mechanical parts performance and fabrication cost. In addition, the topography and texture of the machined surface are used more as an indication of variation in the

tool wear, machine tool vibration, and detection of damaged machine components. Figure 7 shows the topography of a reconstructed three-dimensional hole surface. Roughness includes the finest irregularities of a particular production process or material condition surface. Average roughness (R_a) is the gap between the roughness profile and its centerline, or the function between the absolute value of the roughness profile height and the evaluation length.

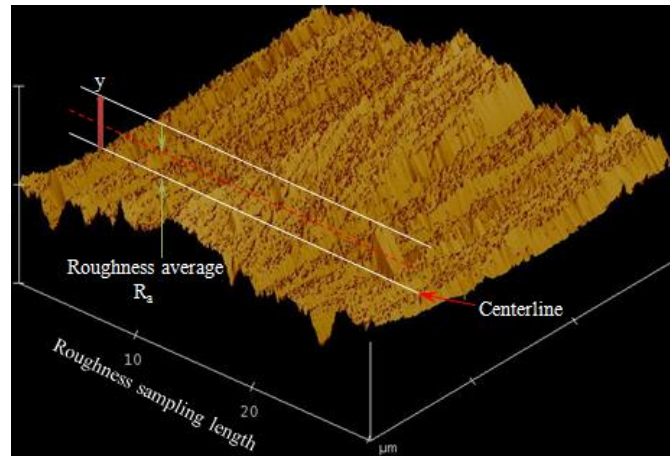


Figure 7: Surface topography and texture during dry drilling of the A356-T0 at 6000 rpm and 0.15 mm/rev

Figures 8 show the generated surfaces by drilling of A356 for cutting speed of 6000 rpm and feed rate of 0.15 mm/rev. In drilling, the tool leaves spiral marks on the machined surface (feed marks). The comparison between different feeds with the same tool shows that the larger feed increases the separation between feed marks, which leads to an increase in the value of the geometric surface roughness. The feed has the main influence on the surface finish obtained. It has been found that the lowest feed values give cheap finish due to very small chip thickness which leads to poor surface formation. Asymmetrical roughness due to plastic deformation was observed when drilling A356 at low cutting speeds. Exceeding a certain value of cutting speed the irregular roughness disappears. Surface roughness at low cutting speeds is influenced by surface plastic deformation and BUE formation. The cutting speed is the parameter which has a great influence on the roughness due to the processed material contribution to the machining process. It becomes dominant in the presence of a BUE and discontinuous chip.

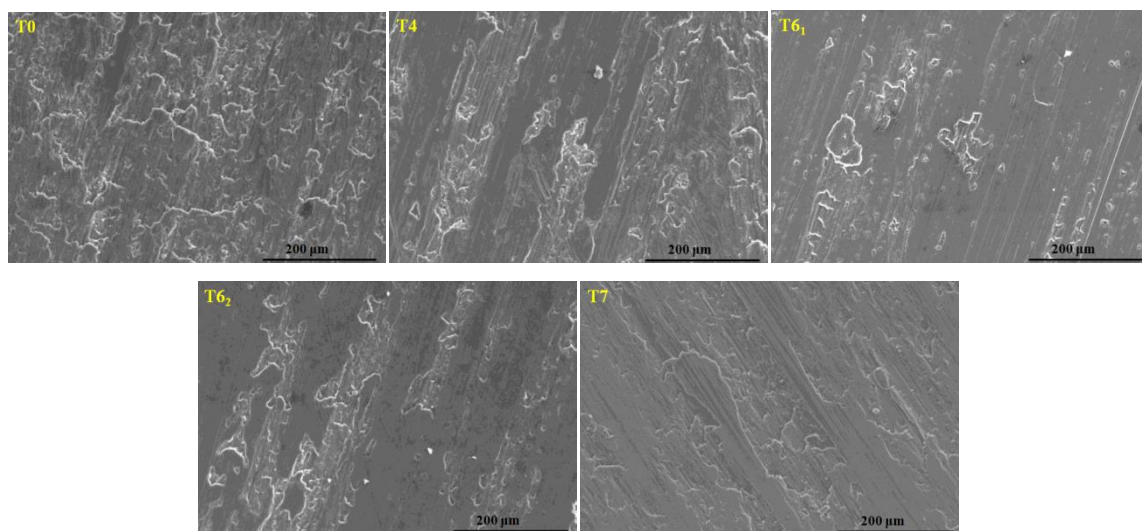


Figure 8. Surface quality on A356 during dry drilling, for cutting speeds of 6000 rpm and feed rate of 0.15 mm/rev as observed with a SEM

The surface roughness values (R_a) of the drilled hole are shown in Figure 9; they are measured parallel to the feed direction. It is evident that surface roughness depends on the machining factors employed each time, which is a complex problem in the drilling process. Commonly, surface roughness is affected by two main factors: the feed and the tool geometry (nose radius). However, in an actual situation as for A356, lubricant modes and heat treatment conditions affect the roughness of machined surfaces. This effect is due to the alteration of parts-tool interactions and the chip formation process. From figure 9, it is confirmed that with an increase of the artificial aging temperature, the values of surface roughness (R_a) are less important. So the heat treatment state is a dominant parameter and has a much more effect on R_a . Heat treatment condition has a much steeper slope than the lubricant modes and it has also observed that the surface roughness showed a variation with the difference of the lubrication mode. As shown clearly in Figure 9, the wet and mist drilling reveal a smoother surface while the dry conditions result in increased roughness. This last condition produces heavily deformed zones on the side-wall with significant feed marks. However, for artificial aging T7, the surface roughness values of holes drilled under wet drilling are almost four times higher than those under mist and dry drilling. It is very important that a wet application was found to have an undesirable effect on the finish of the hole surface. The particular surface effects observed during wet drilling may can be explained by the phenomena of chips dragging against the side wall of the hole as the drill was retracted. The application of high pressure lubrication has trapped the chip within the tool flute which involve that high pressure lubrication is not very efficient. The finest surface quality can be achieved under artificial aging T6 and wet application. Except the artificial aging T7, finest surface quality is resulted under dry drilling than that observed in wet and mist drilling.

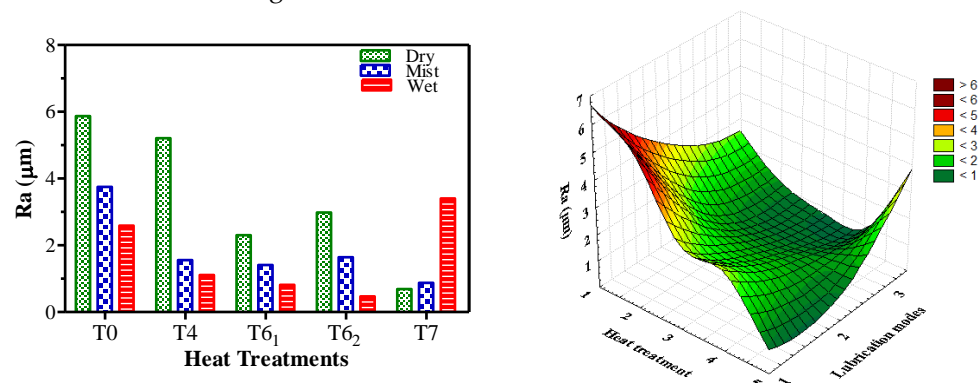


Figure 9: R_a variation under various heat treatments and lubrication modes during drilling of the A356 at 6000 rpm and 0.15 mm/rev

3.5. Burr Formation

In the drilling process, the material extends over the machined surface to exit edges of the part and generates burrs. As a result, most of the burrs are found on the exit surface while the entrance surface of the hole shows small or no burrs. In this case very small burrs were found on the hole edges. These small burrs can be explained by noting that in drilling, the chip load is small at the beginning and end of cut leading to more rubbing instead of cutting. In this study, for different cutting speed and feed rates, the most common burr type observed was a homogeneous burr with a uniform thickness (Figure 10).

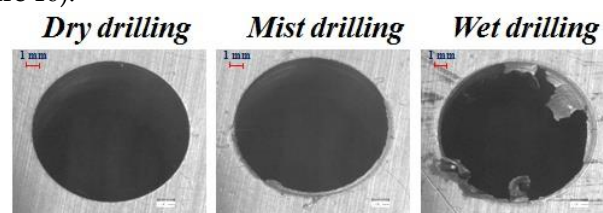


Figure 10. Influence of different cutting fluid on burr formation during drilling of A356-T6 alloy

Figure 11 shows the burr type generated at different heat treatments and cutting speeds during dry drilling of A356 alloy for feed rate of 0.35 mm/rev. Results shows that heat treatment have significant effects on burr height. Figure 12 shows that burr height decreases with T6 heat treatment and then increases with T7 heat treatment. Figure 10 also shows that use of lubricated drilling (mist and wet modes) generates larger burrs compared to dry drilling. Chips formation associated with plastic strain is intensified; this intensification affects the size of the burrs. This is due to the effect of cutting fluid which trims down the temperature in drilling zone, making chip evacuation the process very difficult. On the other hand, using dry cutting condition decreases the burr height. The results show that the heat treatment and the cutting fluid have distinctive effects on the burr size.

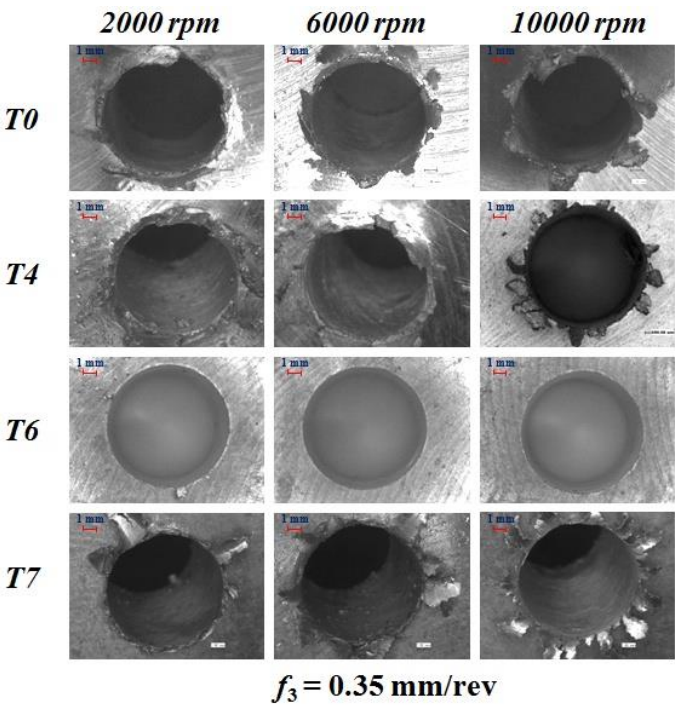


Figure 11. Effect of heat treatments during dry drilling of A356 alloy at different cutting speeds on burr formation

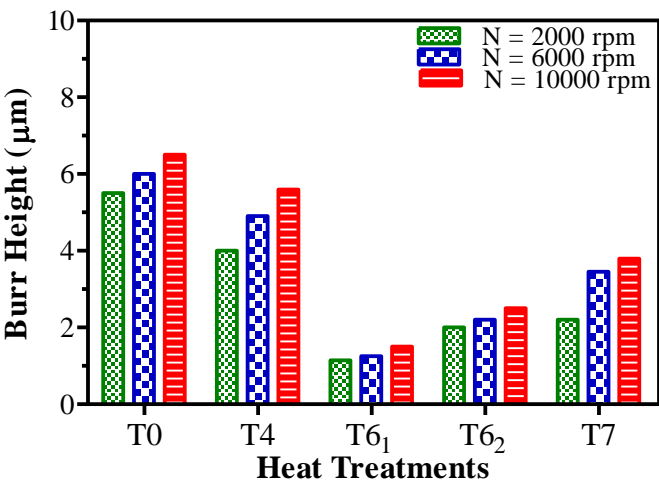


Figure 12. Burr height under various heat treatments at feed rate 0.35 mm/rev

3.6. Tool Wear

Figure 13 show samples of tool flank-wear and BUE formation. In all of the carried out experiments, the major form of tool failure when drilling A356 is flank wear (Figure13). Abrasive wear process while drilling A356 is not at all different from the usual tool wears process when machining metal. This is due to the Si particle abrasion on the tool surfaces during drilling. The major different observed is with the number of Si particle and its size produced by the different solution treatment temperature which became the interest of the tool wears. However, the tool flank-wear was insignificant at the cutting edge. BUE from dry drilling of A356 matrix which is usually soft and ductile is seen in tool flank.

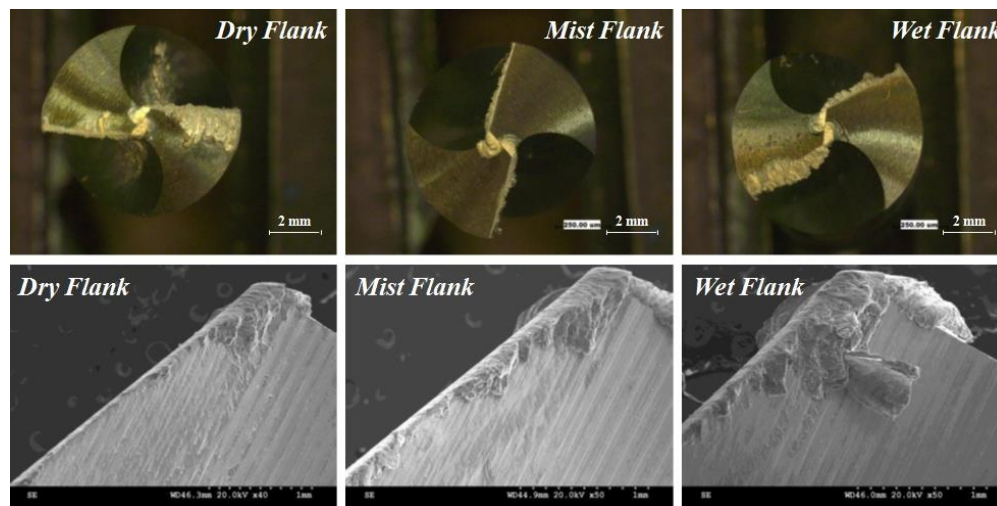


Figure 13. Samples of tool flank-wear and BUE formation

4. Conclusions

The following conclusions were found on experiments conducted to study the effects of heat treatment and lubrication modes on the machinability of Al-Si-Mg cast alloys:

- Heat treatment strongly controls the burr formation and surface quality.
- At low cutting speed we have a better performance of dry drilling and a longer tool life.
- When drilling, better lubrication in the cutting zone can increase tool life and improve surface finish.
- Finest surface quality results when artificial aging at T6 and wet drilling are present.
- Chip formation depends on the heat treatment conditions of the material of the part. Feed rate had the strongest impact on chip formation. The best chip formation was for feed rate at 0.35 mm/rev, dry drilling and artificial aging at T6.

Considering that surface finish of drilled hole wall was most important criteria for drilling process quality, the optimization of cutting conditions for this criterion will be achieved by high feed rate, wet drilling and artificial aging at T6. Although the costs for tools rise, it is still more cost efficient to use more tools than cutting fluids. It is preferable to use dry drilling which generates a higher shear angle (low chip compression ratio). This means a reduction in energy consumption and strain in the chip.

Conflicts of Interest: Declare conflicts of interest or state “The authors declare no conflict of interest.” Authors must identify and declare any personal circumstances or interest that may be perceived as inappropriately influencing the representation or interpretation of reported research results. Any role of the funders in the design of the study; in the collection, analyses or interpretation of data; in the writing of the manuscript, or in the decision to publish the results must be declared in this section. If there is no role, please state “The funders had no role in the design of the study; in the collection, analyses, or interpretation of data; in the writing of the manuscript, or in the decision to publish the results”.

References

1. Akram, Sohail, Imran, Husain, Khan, Mushtaq, et al. A numerical investigation and experimental validation on chip morphology of aluminum alloy 6061 during orthogonal machining. In: 2016 Moratuwa Engineering Research Conference (MERCon). IEEE, 2016. p. 331-336.
2. Demir, Halil et Gündüz, Süleyman. The effects of aging on machinability of 6061 aluminium alloy. *Materials & Design*, 2009, vol. 30, no 5, p. 1480-1483.
3. Zedan Y, Samuel F, Samuel A, Doty H. Effects of Fe intermetallics on the machinability of heat-treated Al-(7–11)% Si alloys. *Journal of Materials Processing Technology*. 2010;210(2):245-57.
4. Demir H, Gündüz S. The effects of aging on machinability of 6061 aluminium alloy. *Materials & Design*. 2009;30(5):1480-3.
5. Songmene V, Masounave J, Balout B. Clean Machining: Experimental Investigation on Dust Formation Part II: Influence of Machining Parameters and Chip Formation, Part II. *Int J Environ Conscious Des Manuf(ECDM)*. 2008;14(1):17-33.
6. Saunders LK, Mauch CA. An exit burr model for drilling of metals. *Journal of manufacturing science and engineering*. 2001;123(4):562-6.
7. Lauderbaugh L. Analysis of the effects of process parameters on exit burrs in drilling using a combined simulation and experimental approach. *Journal of Materials Processing Technology*. 2009;209(4):1909-19.
8. Aurich JC, Dornfeld D, Arrazola PJ, Franke V, Leitz L, Min S. Burrs-Analysis, control and removal. *CIRP Annals - Manufacturing Technology*. 2009;58(2):519-42.
9. Sofronas AS. The formation and control of drilling burrs. PhD Thesis, University of Detroit, USA1975.
10. Hasegawa Y, Shigio Z, Akiyasu Y. Burrs in Drilling and Prevention of it. Technical paper, Society of Manufacturing Engineers, page MR. 1975:75-480.
11. Pande S, Relekar H. Investigations on reducing burr formation in drilling. *International Journal of Machine Tool Design and Research*. 1986;26(3):339-48.
12. Ko S-L, Lee J-K. Analysis of burr formation in drilling with a new-concept drill. *Journal of materials processing technology*. 2001;113(1):392-8.
13. Shivkumar S, Ricci S, Steenhoff B, Apelian D, Sigworth G. An experimental study to optimize the heat treatment of A356 alloy. *AFS Transactions*. 1989;97:791-810.
14. Hetke A, Gundlach R. Aluminum casting quality in alloy 356 engine components. *American Foundrymen's Society, Inc, Transactions of the American Foundrymen's Society*. 1994;102:367-80.
15. Gillespie LRK. Deburring technology for improved manufacturing. Dearborn, MI, USA: Society of Manufacturing Engineers (SME); 1981.
16. Ko S-L. Measurement and effective deburring for the micro burrs in piercing operation. *International Journal of Precision Engineering and Manufacturing*. 2000;1(1):152-9.
17. Wang Q, Cáceres CH, editors. Mg effects on the eutectic structure and tensile properties of Al-Si-Mg alloys. *Materials Science Forum*; 1996: Trans Tech Publ.
18. Djebara, A., Zedan, Y., Kouam, Jules, et al. The effect of the heat treatment on the dust emission during machining of an Al-7Si-Mg cast alloys. *Journal of Materials Engineering and Performance*, 2013, vol. 22, no 12, p. 3840-3853.
19. Callister WD, Rethwisch DG. *Materials science and engineering: an introduction*: Wiley New York; 2007.
20. Jorstad J. Machinability of 380 alloy: effect of minor elements and impurities. *Transactions of the Society of Die Casting Engineers*. 1979;79:072.
21. Jorstad J. Influence of aluminum casting alloy metallurgical factors on machinability. *SAE Technical Paper*, 1980.
22. Burant R, Skingle T. *Machining the Silicon-Containing Aluminum Alloys*. SAE Technical Paper, 1980.
23. Kelly J, Cotterell M. Minimal lubrication machining of aluminium alloys. *Journal of Materials Processing Technology*. 2002;120(1):327-34.
24. Braga DU, Diniz AE, Miranda GW, Coppini NL. Using a minimum quantity of lubricant (MQL) and a diamond coated tool in the drilling of aluminum-silicon alloys. *Journal of Materials Processing Technology*. 2002;122(1):127-38.
25. Klocke F, Eisenblätter G. Dry cutting. *CIRP Annals-Manufacturing Technology*. 1997;46(2):519-26.
26. Zedan Y, Niknam S, Djebara A, Songmene V, editors. Burr Size Minimization When Drilling 6061-T6 Aluminum Alloy. *ASME 2012 International Mechanical Engineering Congress and Exposition*; 2012: American Society of Mechanical Engineers.

27. Niknam SA, Zedan Y, Songmene V. Machining Burrs Formation & Deburring of Aluminium Alloys. Light Metal Alloys Applications 2014. p. 99-122.
28. Sreejith P, Ngoi B. Dry machining: machining of the future. Journal of materials processing technology. 2000;101(1):287-91.
29. Basavarajappa, S.; Chandramohan, G; Narasimha Rao, K V; Adhkrishanan, R; Krish, V.; "Turning of particulate metal matrix composites - review and discussion", Proceedings of the Institution of Mechanical Engineers; Jul 2006; 220, B7; Wilson Applied Science & Technology Abstracts, pp. 1189.